JOURNAL OF MATERIALS SCIENCE **36** (2001) 4045–4057

Conversion of polycarbosilane (PCS) to SiC-based ceramic Part II. *Pyrolysis and characterisation*

HUE QUAN LY, R. TAYLOR, R. J. DAY
Manchester Materials Science Centre, University of Manchester/UMIST, Manchester, M1 7HS, UK
E-mail: richard.day@umist.ac.uk

FRANK HEATLEY
Department of Chemistry, University of Manchester, Manchester, M13 9PL, UK

The conversion to ceramic of a commercial polycarbosilane (PCS) under various pyrolysis conditions has been investigated. The products of pyrolysis have been characterised by solid state ^{29}Si and ^{13}C NMR spectroscopy and X-ray diffraction (XRD). Some of the phases identified in the present study were found to differ from those reported previously, particularly in the earlier literature. Oxidation-cured PCS, when pyrolyzed up to 1400 °C in argon, generally produced silicon oxycarbide (SiO_xC_y) as the second major phase with β-SiC as the major phase, and smaller amounts of free carbon. With increasing temperature above 1200 °C, the silicon oxycarbide phase decomposed to give β-SiC. Silica (SiO_2) was also found to evolve from this silicon oxycarbide phase. Loss of some of the silica, probably by reaction with carbon, was found at 1400 °C, possibly yielding SiO, CO and SiC. At 1500 °C, crystalline α-cristobalite was found as a minor phase with β-SiC as the major phase and a lower amount of free carbon. Pyrolysis in vacuum leads to production and crystallization of β-SiC at a lower temperature than required if pyrolyzed in argon flow. After pyrolysis at 1600 °C in vacuum, the cured PCS converted to almost stoichiometric β-SiC.

1. Introduction

This paper examines the second pyrolysis stage of the conversion of a commercial polycarbosilane (PCS) to ceramic, following the curing stage reported in Part 1 [1].

1.1. Pyrolysis process

The conversion of PCS to ceramic is generally attained by heating the precursor polymer to temperatures above 1000 °C in an inert atmosphere. This pyrolytic conversion process of PCS and oxidation-cured PCS has been found to involve a number of stages [2–4]. During pyrolysis up to ca. 800 °C, degradation of low molecular weight molecules and decomposition of organic side groups occurs. Large weight losses and gaseous evolution of mainly H_2 and CH_4 are associated with these reactions. Si-H and C-H bonds are readily broken. With increasing temperature, connectivity of Si-C-Si bonds increases and a network structure can form via condensation reactions between CH_4 and CH_3 units [2]. In the pyrolysis residue after 700 °C, the presence of C=C bonds has been confirmed, possibly arising from dehydrogenation in -CH-CH- fragments [5]. The increase in density is most rapid between ca. 550 and 800 °C, when the organic PCS transforms into a more inorganic state [2]. By 800 °C, this transition is essentially complete and an amorphous residue is obtained. Soraru *et al*. [6] reported the presence of hydrogen as CH groups in this amorphous residue. Oxygen introduced in oxidation-cured PCS is not eliminated by this stage of pyrolysis [3]. Absence of this oxygen is expected in uncured PCS, whereas none was mentioned by Soraru *et al*. [6], Si-O bonds were reported by Hasegawa and Okamura [2] and Bouillon *et al*. [7]. Residual CH or CH_2 units in the amorphous residue decompose with increasing temperature but the structure remains amorphous below 1000 °C. In the pyrolysis of uncured PCS between 1000 and 1200 °C, β-SiC microcrystals begin to nucleate from the amorphous matrix of Si, C, O and H accompanied by evolution of H_2 gas. The presence of excessive hydrogen could delay this process [8]. Monthioux and Delverdier [9] found that carbon always nucleates first, as basic structural units (BSUs) which are small stacks of 2–3 polyaromatic layers about 1 nm in lateral extension. The presence of oxygen atoms would not favour this nucleation. The periphery of these carbon atoms is thought to be saturated with hydrogen atoms which, in the 1000 to 1200 °C range, are removed mainly as H_2 gas. This release of H_2 induces an edge-to-edge

association of BSUs into larger stacks. SiC was found to be the second phase to nucleate due to structural rearrangements at the solid state within the remaining Si-C-O phase. This was considered to occur concomitantly with the edge-to-edge association of the BSUs. The evolution from uncured PCS between 1000 and 1200 °C did not occur in the pyrolysis of cured PCS, thus the oxygen introduced by the curing process is thought to suppress crystallization of the β-SiC [10]. Above 1200 °C, crystallization of β-SiC continues with slow crystal growth for the uncured PCS, while it is the beginning of crystallization for the cured PCS. In the case of cured PCS, hydrogen evolution is not reported with the crystallization of β-SiC from the amorphous matrix [3, 7]. Instead, crystallization is accompanied by CO gas evolution. Thus, this CO gas could be due to carbothermal reduction of oxygen bonds which is linked to the oxidation curing process. Bouillon *et al*. [11] reported the amorphous to crystalline transition for the cured PCS and suggested that the main gaseous product should be SiO with a lower proportion of CO. The production of SiO and CO should be the result of decomposition of the amorphous Si(C,O) phase. Crystal growth of the β-SiC is suggested to be the result of the reaction of the carbon and Si-O species at the β-SiC grain boundaries. The precipitation of carbon particles from the carbon-rich Si(C,O) phase may compete with the loss of carbon by reaction with Si-O species [12]. The precipitation rate is higher than the loss rate up to 1400 °C. At ca. 1500 °C, the loss rate of carbon is higher than the gain in carbon precipitation, and the amount of free carbon decreases with increasing temperature.

1.2. Microstructure

Several complementary techniques have been used to study the microstructure of commercial PCS-derived Nicalon fibres, including infrared spectroscopy, solid state NMR [13, 14], X-ray diffraction (XRD) [15], transmission electron microscopy (TEM) [16] and Raman spectroscopy [12, 17]. Solid state NMR has an advantage over the other techniques in that it is a bulk sensitive technique representative of the entire sample under study, whereas traditional techniques such as XRD are dependent upon the sampling depth [18].

The composition of Nicalon fibre made by the pyrolysis of oxidation-cured PCS fibre to 1300 °C in inert atmosphere is non-stoichiometric ($SiC_{1.22}O_{0.33}H_{0.10}$) [19]. Earlier reports indicated the presence of amorphous SiO_2 shown by Raman spectroscopy [12] or crystalline SiO_2 evident by XRD [2], microcrystalline carbon [12] as well as the predominant phase of β-SiC which appeared amorphous on TEM micrographs but was considered as microcrystals due to presence of a weak but visible XRD pattern. β-SiC microcrystal sizes in the range of 1 to 10 nm have been obtained by TEM studies [20, 21]. The β-SiC crystallite size was smaller for a fibre with higher oxygen content [22]. As with earlier reports [23, 24], the Nicalon fibre was assumed to consist of stoichiometric phases, with a typical composition by weight of 65% SiC, 20% SiO_2 and 15% free carbon [25]. However, more recent studies have proposed that a non-stoichiometric silicon oxycarbide, SiO_xC_y, is present in the Nicalon fibre. Porte and Satre [26] proposed this ternary phase based upon the results of X-ray photoelectron spectroscopy which showed a peak at a binding energy intermediate between that of SiO_2 and SiC. Using extended X-ray absorption fine structure (EXAFS), NMR spectroscopy, and additional methods, Laffon *et al*. [27] concluded that β-SiC is embedded in a continuum of tetrahedral SiC_xO_y, where $x + y = 4$. In addition, free aromatic carbon aggregates are inserted within the tetrahedral continuum. This model was found to be in agreement with later work by others [28–30]. There is also a general conclusion that SiO_2 is only confined on the fibre surface, and is formed during industrial preparation of the fibre [28]. A quantitative approach was made by Le Coustumer *et al*. [30] based on TEM and elemental analysis. It was concluded that Nicalon fibre is composed of, by weight, 55% β-SiC microcrystals (1.6 nm), separated from each other by 40% $SiO_{1.15}C_{0.85}$ phase acting as grain boundaries, and 5% free carbon which is also an intergranular phase, made of basic structural units (0.8 nm diameter entities of 2 aromatic planes stacked face to face) located at random. Recent work by Hahn *et al*. [31] showed that carbon is also distributed within the oxycarbide phase. With increasing temperature, the carbon reorganizes into a network chain structure. By embedding in the amorphous glassy oxycarbide phase, the free carbon is not readily exposed to oxidation [32]. There are no known equilibrium solid phases between SiC and SiO_2 [33], but the existence of metastable silicon oxycarbide phases has been reported. This SiO_xC_y phase was found at the interface between SiC and SiO_2 surface layer formed during the oxidation of the SiC [34]. Silicon oxycarbide glasses have been obtained by pyrolysis of silicone polymers [35] and silica-based gels [36]. There is no mention of any direct carbon-oxygen bonds in the SiO_xC_y phase in the literature. Renlund *et al*. [37] found no evidence for C-O bonds. Corriu *et al*. [38] assumed that all the carbon atoms in the oxycarbide phase are bonded to Si atoms only and so described the SiO_xC_y phase as a random network of CSi_4 tetrahedra with Si-O-Si bridges. This random network resulted from redistribution reactions involving the exchange of Si-O bonds with Si-C bonds during the pyrolysis of the cross-linked silicone polymer before degradation of the organic groups (500–600 °C). The presence of the grain boundary SiO_xC_y phase meant that, below its decomposition temperature (ca. 1300 °C), crystallization and growth of β-SiC is delayed [39]. Above this degradation temperature, the intrinsic oxygen has a catastrophic effect, i.e., oxidation of the intergranular carbon and a drastic secondary crystal growth because the SiC grains are free to coalesce.

The effect of the extent of curing on the pyrolysis residue is presented in this paper. Products of cured PCS pyrolyzed to different temperatures under argon and vacuum have been followed in some detail, particularly by solid state nuclear magnetic resonance spectroscopy. The thermal expansion behaviour of cured PCS has also been followed.

TABLE I Pyrolysis of as-received (uncured) and cured PCS. All samples were heated from and cooled to room temperature

	Conditions						
	Cure (in air)			Pyrolysis			
Sample	Heating/Cooling rate (°Ch^{-1})	Final Temp. (°C)	Hold time (h)	Heating/Cooling rate (°Ch^{-1})	Final Temp. (°C)	Hold time (h)	Atm.
P1	Not applied			100	1000	1	Ar
C1P1	10	200	0.5	100	1000	1	Ar
C2P1	10	200	1.0	100	1000	1	Ar
C3P1	10	200	1.5	100	1000	1	Ar
C4P1	30	200	1.0	100	1000	1	Ar
C2P12	10	200	1	100	1200	1	Ar
C2P14	10	200	1	100	1400	1	Ar
C2P15	10	200	1	100	1500	1	Ar
VC2P10	10	200	1	100	1000	1	Vacuum
VC2P12	10	200	1	100	1200	1	Vacuum
VC2P16	10	200	1	100	1600	1	Vacuum

2. Experimental

2.1. Pyrolysis

A summary of the pyrolysis work carried out and the corresponding sample identification is shown in Table I. All pyrolysis experiments were carried out at a heating/cooling rate of 100 °C h^{-1} to the desired temperature. The hold time at the final heat treatment temperature was fixed at one hour. All samples were pyrolyzed in an alumina crucible except for sample VC2P16, where a graphite crucible was used to avoid reaction between the alumina and sample at high temperatures.

2.1.1. Pyrolysis of cured PCS in argon

To obtain the effect of the extent of curing on the pyrolysis residue, 2 g samples cured under conditions C1 to C4 (Table I), described in the previous paper [1], were pyrolyzed to 1000 °C, giving products C1P1, C2P1, C3P1 and C4P1, respectively (Table I). In another set of experiments, PCS samples (ca. 5 g) were cured according to the conditions of C2 (heating/cooling rate at 10 °C h^{-1}, final hold at 200 °C for 1 h) and then pyrolyzed to 1200 °C, 1400 °C and 1500 °C, giving products C2P12, C2P14 and C2P15, respectively. All pyrolyses were carried out in an alumina tube furnace which was purged with argon prior to and during pyrolysis. The total impurities of oxygen and water in argon were 6 ppm. Samples C2P12 to C2P15 were pyrolysed in a larger furnace than that used for samples C1P1 to C4P1, otherwise the same argon atmosphere was used.

2.1.2. Pyrolysis of cured PCS in vacuum

PCS samples (ca. 5 g) also cured to the C2 condition were pyrolyzed in vacuum (ca. 10^{-6} atm) using a carbon heating element furnace. Cured samples were pyrolyzed to 1000, 1200 °C in an alumina crucible and to 1600 °C in a graphite crucible, giving samples VC2P10, VC2P12 and VC2P16, respectively.

2.1.3. Pyrolysis of as-received PCS

About 2 g of as-received PCS was directly pyrolyzed to 1000 °C in argon without prior curing (P1) to compare with the oxidation cross-linked products.

2.2. Characterisation of pyrolysis products

The pyrolysis yield was determined as the weight of the pyrolysis residue expressed as a percentage of the weight of the initial precursor. Elemental analysis was carried out on the pyrolysis products for Si, C, H and O (by difference)

2.2.1. Solid state ^{29}Si and ^{13}C NMR spectroscopy

^{29}Si and ^{13}C NMR spectra were obtained using a Varian Associates Unity 300 spectrometer, operating at 59.7 MHz for ^{29}Si and 75.5 MHz for ^{13}C. Powdered PCS of about 0.5 g was packed into a zirconia sample holder. The magic angle spinning (MAS) technique was applied to reduce the line broadening due to the range of molecular orientations in the magnetic field. The spinning frequency was ca. 4 to 5 kHz. For the samples where carbon or silicon nuclei are bonded with, or in close proximity to, protons, the cross polarization (CP) technique is normally applied, as in Part 1.[1] This involves generation of a ^{29}Si and ^{13}C signal indirectly by transfer of magnetization from protons, so that better signal to noise ratios are obtained compared to the alternative direct excitation (DE) method in which a ^{29}Si and ^{13}C signal is generated by application of an exciting pulse at the ^{29}Si and ^{13}C resonance frequency. As described below, the DE technique was principally used in this work because of the low concentration of protons in the pyrolyzed samples. The chemical shift reference was tetramethylsilane (TMS) for both ^{29}Si and ^{13}C.

2.2.2. X-ray diffraction

X-ray diffraction was performed using a Philips X'PERT APD diffractometer equipped with a programmable unit. Copper K_a radiation of wavelength 0.15417 nm was used. A continuous scan from $2\theta = 5°$ to 80° was carried out at a scan rate of 0.016° s^{-1}.

2.2.3. Dilatometry

The thermal expansion behaviour in argon of a compacted sample of cured (C2 condition) PCS was followed by the pushrod dilatometry method. The sample

was heated from room temperature up to 1200 °C with a 1 hour hold and then cooled to room temperature. The heating/cooling rate was 100 °C h^{-1}, i.e., simulating the conversion condition of C2P12 (Table I). The specimen for thermal expansion measurement was prepared by pressing ca. 0.2 g of the cured PCS in an 8 mm diameter die, under about 80 MPa pressure for 1.5 min at room temperature, producing a disc about 3 mm in length. Measurements were made transverse to the plane of pressing of the sample at 3 °C intervals. A horizontal alumina pushrod dilatometer assembly was used, which uses a linear variable differential transducer to detect length changes.

3. Results and discussion

3.1. Analysis of pyrolysis products

3.1.1. Preliminary discusion of NMR spectra

Before discussing the pyrolysis results in detail, it is worthwhile describing some general features of the NMR results because of their significance in applying and interpreting the NMR technique. For this, sample C2P1 is used as an example. Figs 1 and 2, respectively show ^{29}Si and ^{13}C spectra obtained for this sample using a variety of techniques and conditions. In both Figures, a significant feature is the much greater intensity of DE spectra compared to CP spectra (cf. Figs 1a and b, and 2a and b), due to the very low proton content of the pyrolyzed samples. Furthermore, in ^{29}Si spectra, several peaks were observed (assigned below) whose relative intensity of the peaks depended significantly on whether DE or CP was used. Provided a sufficient pulse interval is used, DE spectra give reliable relative intensities, so for this reason, as well as the greater intensity, DE was used for all other NMR spectra reported here with a pulse interval of at least 60 s. Comparison of Fig. 1a and b shows that the peaks at −70 and −110 ppm were relatively much weaker in CP spectra than the peak at −10 ppm and the shoulder at −35 ppm. The peaks at −10 and −35 ppm must, therefore, arise from ^{29}Si nuclei closer to protons.

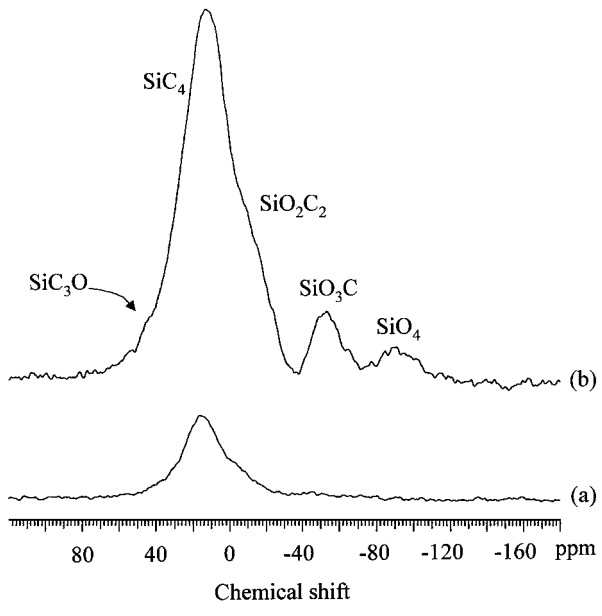

Figure 1 ^{29}Si MAS spectra of C2P1. (a) DE spectrum; (b) CP spectrum (contact time 2 ms).

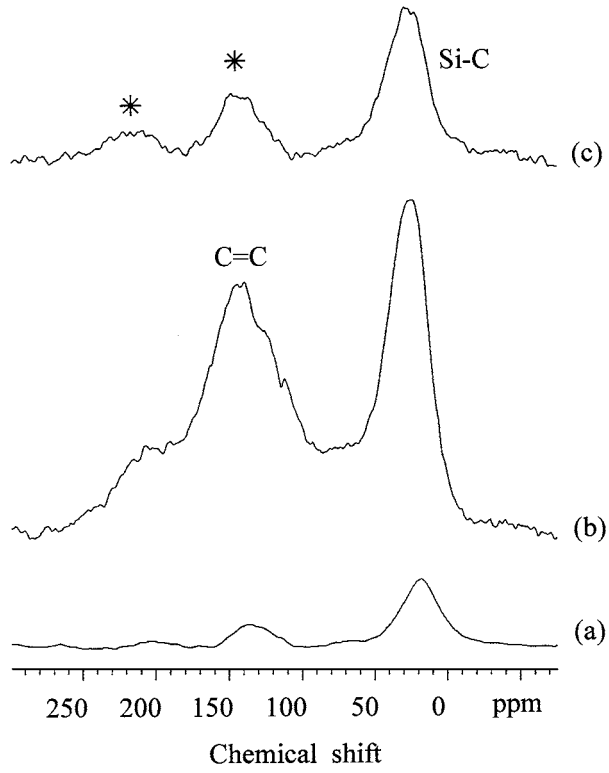

Figure 2 ^{13}C MAS spectra of C2P1. (a) DE spectrum; (b) CP spectrum (contact time 2 ms); (c) DE spectrum with a dipolar dephasing interval of 40 μs (see text). * denotes a CSA spinning sideband.

In ^{13}C DE spectra (Fig. 2a), a large, broad background peak was observed centred at ca. 140 ppm which severely obscured the small peak at the same position observed in the CP spectrum (Fig. 4b); this peak was assigned to unsaturated structures. The presence of this peak in the DE spectrum was revealed by its high frequency chemical shielding anisotrophy (CSA) spinning sideband at ca. 210 ppm; a similar low frequency sideband would be expected at ca. 70 ppm. A much more intense peak assigned to saturated carbon species was clearly observed in both DE and CP spectra at ca. 20 ppm. The background peak arose from fluorinated polymer used as a housing for the MAS stator, and was not observed in CP spectra because of the absence of protons in the polymer. Although the background resonance severely hindered analysis of ^{13}C spectra, its effect was mitigated by the fact that the ^{13}C spectra were not very informative about the pyrolyzate structures. The background peak was substantially eliminated by a dipolar dephasing spectrum (Fig. 4c) in which ^{13}C signals are allowed to decay under the influence of dipole–dipole interactions before detection. However this technique also significantly attenuated the saturated ^{13}C peak at 20 ppm, indicating that those carbons were in general much closer to protons than the unsaturated carbons.

3.1.2. Pyrolysis of as-received PCS

When as-received PCS was pyrolyzed to 1000 °C in argon without prior curing (P1), a black expanded product was obtained. This highly porous structure is due to the loss of organic oligomers and gaseous by-products

TABLE II Chemical composition (wt%) and empirical formula of as-received PCS pyrolyzed to 1000 °C without prior curing

Sample	Si	C	H	O	Empirical formula
P1	54.6	33.7	-	11.7	$SiC_{1.48}O_{0.38}$
as-received PCS [1]	43.7	40.8	8.3	7.2	$SiC_{2.2}H_{5.3}O_{0.3}$

on pyrolysis [40]. The pyrolysis yield was found to be 69.6 wt%. Elemental analysis of the product (Table II) showed a reduction in the carbon content compared to the initial PCS, probably due to the loss of organic side groups. Relative to stoichiometric SiC, an excess of carbon was indicated but no hydrogen was detected. The amount of oxygen increased after pyrolysis possibly due to incorporation of oxygen into the structure replacing the organic groups lost on pyrolysis.

Fig. 3a shows the DE/MAS ^{29}Si NMR spectrum of sample P1. The main peak at −12 ppm was close to reported values of around −15 ppm, characteristic of silicon sites in amorphous β-SiC [4, 5]. The presence of a small number of SiO_4 units was also indicated by the signal at ca. −100 ppm which has been reported to be characteristic of a silica (SiO_2) phase [41].

The ^{13}C DE/MAS spectrum of sample P1 (Fig. 3b) showed a major resonance peak at +19 ppm. This may be due to Si_4C sites in β-SiC, but any saturated C-H environments would also resonate in this region [8]. However no hydrogen was detected in the elemental analysis. Variable spinning speed experiments and comparison with the spectrum of an empty rotor showed that the small peak at ca. +185 ppm was a CSA spinning sideband of a C=C resonance at +120 ppm which was assigned to aromatic C=C bonds [42]. These C=C structures have been reported to be precursors for graphitic carbon which is formed at ca. 1200 °C [6].

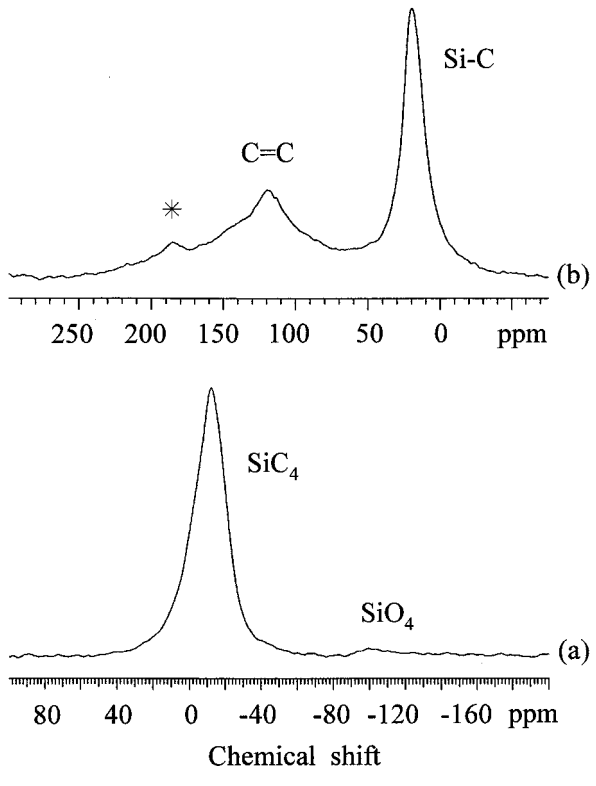

Figure 3 DE/MAS spectra of P1. (a) ^{29}Si spectrum; (b) ^{13}C spectrum. * denotes a CSA spinning sideband.

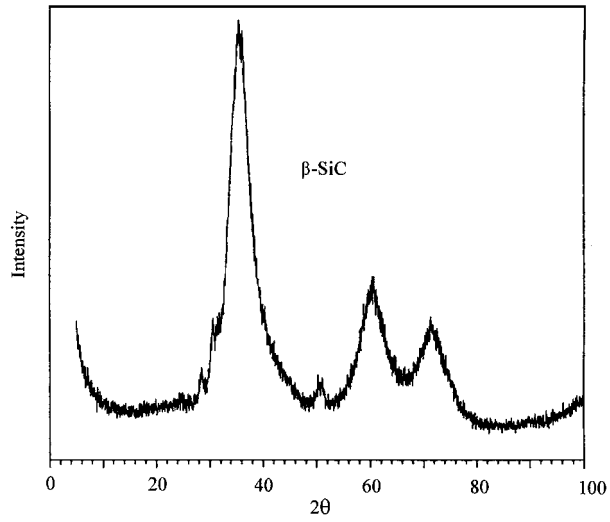

Figure 4 XRD pattern of P1.

Fig. 4 shows the X-ray diffraction pattern of sample P1. The three most intense peaks at $2\theta = 36$, 60 and 72° corresponded respectively to the diffraction lines from the (111), (220) and (311) lattice planes of β-SiC according to the standard Hanawalt pattern for polycrystalline β-SiC. The diffraction peaks were relatively broad compared to standard XRD patterns for crystalline β-SiC, suggesting an amorphous nature for the β-SiC. The silica and free carbon suggested by the ^{29}Si and ^{13}C NMR spectra were not reflected in the XRD pattern, possibly due to their amorphous nature.

Table III gives a comparison of the products obtained in this study to those obtained by other authors where a similar PCS precursor and pyrolysis conditions were used. The quantity of these phases, however, could not be determined from the present results. Calibration of the NMR peaks using standard samples of β-SiC, SiO_2 and carbon may permit quantification. Compared to the findings of Soraru *et al*. [6] where pyrolysis was carried out in argon as in the present study, amorphous SiO_2 was found in the present study whereas none were reported in the literature where residual hydrogen was found. The origin of these differences may lie in differences in PCS precursor state or thermal histories.

3.1.3. Pyrolysis of cured PCS in argon

Since direct pyrolysis of PCS without prior curing resulted in an expanded foam residue, which has been reported to be caused by high volatilization of oligomers [40], a curing treatment prior to pyrolysis was needed to cross-link the PCS. Cure by heating in air was carried out. Samples C1, C2 and C3 were obtained by curing at a heating rate of 10 °C h^{-1} to 200 °C, with a hold time of 0.5, 1, and 1.5 h, respectively. Sample C4 was obtained by curing at a heating rate of 30 °C h^{-1} to 200°C with a hold time of 1 h. Samples of PCS cured under conditions C1 to C4 were then pyrolyzed to 1000 °C in argon. With curing before pyrolysis, there was no foaming in the pyrolytic residue and the original shape of the precursor was retained reasonably well. The resulting pyrolytic yields are shown in Table IV. Compared to

TABLE III Summary of products found in the experimental study compared to those in the literature (■ amorphous, ❒ semi-crystalline, □ crystalline)

Conditions	Found in experiment		Reported in literature	
	Temp. (°C)	Products	Temp. (°C)	Products
As-received PCS in argon				
	1000	❒ β-SiC (major), ■ SiO_2 (minor), Free C (minor).	1000	■ β-SiC (major), Free C (minor), Residual H (trace) [6].
	1000	■ β-SiC (major), SiO_xC_y (major), Free C (minor), Residual H (trace).		–
	1200	■ β-SiC(major), SiO_xC_y (major), Free C (minor).	1250 to 1350	β-SiC (major), SiO_xC_y (major), Free C (minor) [20, 52].
Cured PCS in argon				
	1400	❒ β-SiC (major), SiO_xC_y (medium), ■ SiO_2 (minor), Free C (minor).	–	–
	1500	❒ β-SiC (major), SiO_xC_y (trace), ■ & □ α-Cristobalite (minor), Free C (trace).	–	–
	1000	■ β-SiC (major), SiO_xC_y (medium), Free C (minor), Residual H (trace).	1000	■ β-SiC, ❒ SiO_2 <quartz>, Free C [3].
	1200		1200	■ β-SiC, □ SiO_2 <quartz>, Free C [3].
Cured PCS in vacuum		❒ β-SiC (major), SiO_xC_y (minor),	–	–
	–	■ α-cristobalite (minor), Free C (minor).		–
	1600	– □ β-SiC (major), Free C (trace).		

TABLE IV Effect of cure conditions on the yield after pyrolysis to 1000 °C in argon

Sample	Heating rate (°Ch^{-1}) at 200 °C & Cure time (h)	Pyrolysis yield (%)
C1P1	10, 0.5	91.1
C2P1	10, 1.0	91.4
C3P1	10, 1.5	91.7
C4P1	30, 1.0	88.8

TABLE V Chemical composition (wt.%) and empirical formulae of the various cured PCS pyrolyzed to 1000 °C in argon

Sample	Si	C	H	O	Empirical formula
C1P1	53.3	30.2	0.2	16.3	$SiC_{1.32}H_{0.11}O_{0.54}$
C2P1	51.4	30.3	0.6	17.7	$SiC_{1.38}H_{0.27}O_{0.61}$
C3P1	50.9	29.6	0.6	18.9	$SiC_{1.36}H_{0.33}O_{0.65}$
C4P1	53.9	32.5	0.1	13.5	$SiC_{1.41}H_{0.05}O_{0.44}$

a yield of 69.6 wt.% for direct pyrolysis without prior curing, results of Table IV shows that the ceramic yield was enhanced with cross-linking of the PCS precursor before pyrolysis. The yield of sample C4P1 was lowest since the extent of curing prior to pyrolysis was lowest. As expected, the residual yield was slightly increased between samples C1P1 to C3P1, reflecting the time allowed to cure which increased in this order, reducing the loss of PCS fragments because of the cross-linking with oxygen.

Elemental analyses of the pyrolytic residues C1P1 to C4P1 are shown in Table V. Compared with the results for sample P1 (Table II) where no prior curing was applied, it appeared that the oxidation curing step had an inhibiting effect on the loss of hydrogen during pyrolysis. This effect increased with the extent of curing. Due to the additional oxygen introduced by the curing process, the amount of residual oxygen also increased for the cured samples. There appeared to be some variation in the carbon content which showed no clear trend in the amount of residual carbon with the extent of curing. It has been reported that the C/Si ratio would tend to be lower with oxidation curing [43], due to removal of some carbon by the oxygen with release of oxides of carbon. Variations in the distribution of carbon in the sample, the chemical bonding and reactivity of the carbon on analysis may affect the amount of carbon detected. For samples that had been cured, excess carbon is more likely to be incorporated within the glassy amorphous silicon oxycarbide structure whereas for a non-oxidation cross-linked sample, excess carbon

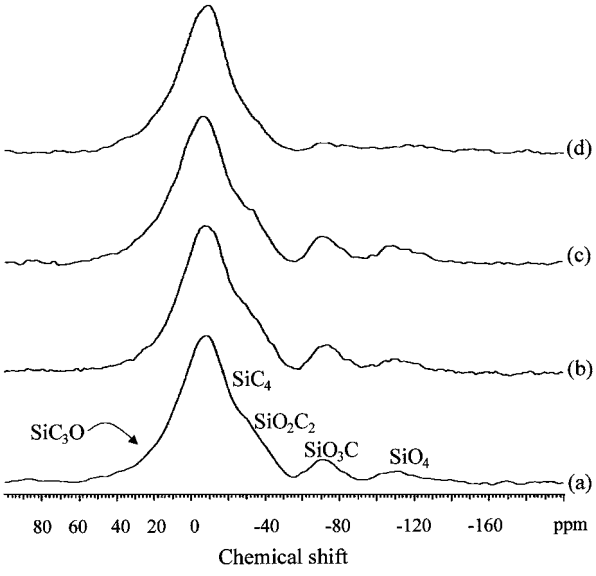

Figure 5 ^{29}Si DE/MAS NMR spectra of (a) C1P1; (b) C2P1; (c) C3P1; (d) C4P1.

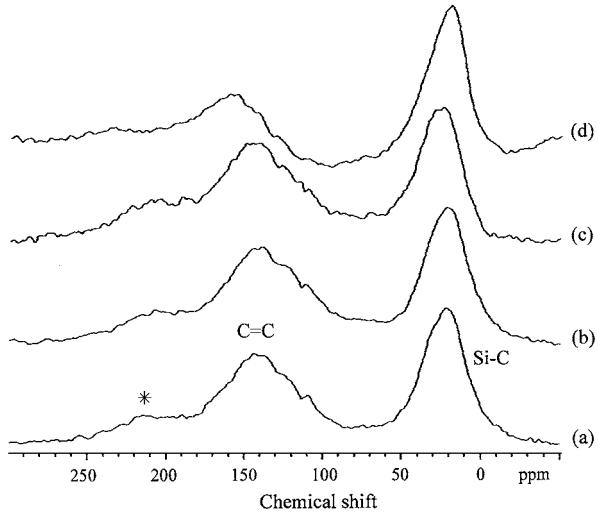

Figure 6 ^{13}C DE/MAS NMR spectra of (a) C1P1; (b) C2P1; (c) C3P1; (d) C4P1. * denotes a CSA spinning sideband.

is expected to separate out as free carbon in the pyrolytic residue [43, 44]. The amount of oxygen in the residues was found to increase with the extent of curing as expected.

^{29}Si DE/MAS NMR spectra of samples C1P1 to C4P1 are shown in Fig. 5. In the spectra of samples C1P1 to C3P1, four characteristic chemical shifts were observed, suggesting four different Si environments. These peaks have been identified using known shifts for various silicon carbide polymorphs, silica, silicon oxycarbide glasses and carbon [6, 8, 14, 18, 42, 45–47]. The major peak at about −9 ppm was due to SiC_4 units indicative of an amorphous hydrogenated silicon carbide phase. Compared to a value of −12 ppm for sample P1 where no prior curing was applied, there was a shift towards positive values in the chemical shift as the silicon carbide became more hydrogenated and amorphous. This peak also appeared to overlap with a signal about −30 ppm due to SiO_2C_2 units. This −30 ppm peak became more separated from the main peak at −9 ppm as the extent of curing increased as in sample C3P1. A shoulder at about +20 ppm under the SiC_4 main peak may indicate the presence of $SiOC_3$ units [18]. The signals at around −72 ppm and −110 ppm were assigned to SiO_3C and SiO_4 units, respectively. Random arrays of these $SiOC_3$, SiO_2C_2, SiO_3C, SiO_4 and SiC_4 units have been considered to be the amorphous silicon oxycarbide phase [47]. The majority of the SiC_4 units, however, have been found to belong to the separate β-SiC phase [27]. The SiO_4 units have also been assigned to silica [46] although more recent reports [27, 38, 47] considered the SiO_4 units to be incorporated within the silicon oxycarbide phase below 1400 °C. Thus, the SiO_4 units are assumed to be part of the silicon oxycarbide (SiO_xC_y) phase rather than a separate silica phase. Overall, the relative proportions of the various phases appeared similar between samples C1P1 to C3P1, i.e., with a cure time of 0.5, 1.0 and 1.5 h, respectively. In the spectrum of sample C4P1 where the extent of curing was least, the main peak at −9 ppm due to SiC_4 units appeared as in the spectra of samples C1P1 to C3P1 but the signals due to units of $SiCO_3$ (+20 ppm), SiO_2C_2 (−30 ppm), SiO_3C (−73 ppm) and SiO_4 (−110 ppm) were weak because the amount of oxygen incorporated into this sample during curing was lowest.

In the solid state ^{13}C DE/MAS spectra of samples C1P1 to C3P1 (Fig. 6), the peak at around +20 ppm was due to the presence of the amorphous β-SiC phase. As the extent of curing increased, the position of this signal tended to shift slightly to higher values, from about +20 ppm to about +25 ppm. The ^{13}C chemical shifts have been found to move to higher values when the number of protons bonded to carbon increases [8]. Thus, the shift of the peak due to amorphous silicon carbide at around +20 ppm in sample C4P1, to a higher value at about +25 ppm in sample C3P1, is likely to be due a more hydrogenated carbide residue with increase in the extent of curing. This is in agreement with the result found for sample P1 where no residual hydrogen was shown, and a lower chemical shift (+19 ppm) was seen (Fig. 2). The peak at 210 ppm was assigned to a CSA spinning sideband of unsaturated carbons at ca. 140 ppm. These NMR results suggest that pyrolysis of cured samples C1 to C4 produces mainly amorphous β-SiC, with a silicon oxycarbide phase as the second major phase, and smaller amounts of free carbon.

The XRD patterns for samples C1P1 to C4P1, shown in Fig. 7, all showed similar features. All the cured and pyrolyzed samples showed no separation of the (220) and (211) diffraction peaks of β-SiC, and the line widths were broad compared to that of sample P1 (Fig. 4) where no prior curing was applied. This indicated that the oxidation curing treatment resulted in a suppression in the crystallization of the β-SiC. The free carbon phase suggested by ^{13}C NMR was not observed in these XRD patterns, probably because of its amorphous state. The delay in the ordering of the β-SiC phase is thought to be due to the residual hydrogen and oxygen, where the residual Si-O and C-H bonds hinders the formation of a regular three dimensional Si-C network [9, 48].

Overall, the above results showed that oxidation curing the as-received PCS before pyrolysis produces a

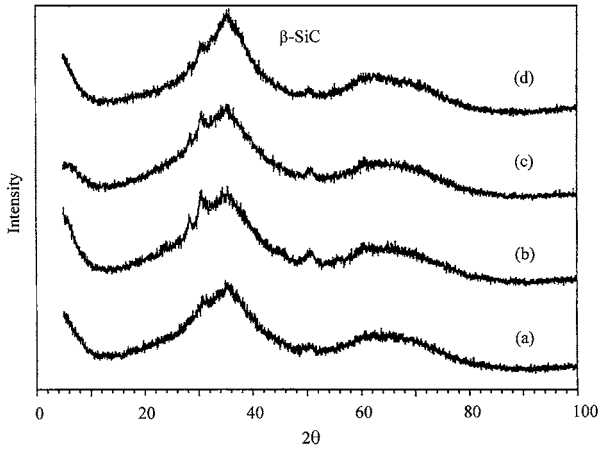

Figure 7 XRD patterns of (a) C1P1; (b) C2P1; (c) C3P1; (d) C4P1.

silicon oxycarbide phase and residual hydrogen in addition to the β-SiC, SiO_2 and free carbon formed when as-received PCS was pyrolyzed without prior curing. It appeared that the SiO_4 units may exist as a separate silica phase in the pyrolysis of uncured PCS whereas the SiO_4 units exist within the silicon oxycarbide product of pyrolysis of cured PCS. The residual hydrogen has been considered to be linked to the periphery of carbon atoms [9]. Thus, the structure of the pyrolysis product of oxidation-cured PCS may be similar to that proposed for the structure of the PCS-derived Nicalon fibre by Laffon *et al*. [27]. In this model, the silicon carbide grains or crystals are surrounded by the silicon oxycarbide phase, a random distribution of $SiOC_3$, SiO_2C_2, SiO_3C, SiO_4 and SiC_4 units. The unsaturated carbon may exist as free aromatic carbon between the silicon carbide and silicon oxycarbide tetrahedral continuum. The residual hydrogen atoms may surround some of these aromatic carbon units. The commercial Nicalon fibre used in their study was believed to be manufactured using an oxidation curing process and pyrolysis at around 1300 °C in nitrogen. Work using the same cure and pyrolysis conditions and a similar PCS was not found in the open literature to allow for comparison. The closest reported conditions used were those by Hasegawa [3], where PCS cured at 190 °C in air was pyrolyzed at 1000 °C in vacuum. Table III summarizes the products found in that author's work and the present work. Like other earlier reports, the silicon oxycarbide (SiO_xC_y) phase suggested by ^{29}Si NMR in the present study was not mentioned in Hasegawa's work [3], whereas crystalline SiO_2 (quartz) was generally reported where XRD was mainly used to identify the phases [2, 3, 49]. The above results in this study showed that there were no significant changes in the products with increasing cure time of 0.5, 1.0 and 1.5 h at 200 °C. This suggests that a cure time of 0.5 hour may be sufficient to stabilize the PCS before high temperature pyrolysis and also give a reasonable ceramic yield, although at the expense of introducing the metastable SiO_xC_y phase.

C2-cured PCS samples pyrolyzed in argon up to 1200 (C2P12), 1400 (C2P14) and 1500 °C (C2P15) were also characterized. Pyrolysis yields are shown in Table VI. The pyrolysis yield decreased with increasing pyrolysis temperature as expected. Comparing these results with those of Table IV, it can be seen that although samples C2P12 to C2P15 were pyrolyzed to higher temperatures, their yields were higher than those of samples C1P1, C2P1 and C3P1 where a lower pyrolysis temperature of 1000 °C was used, as well as a higher extent of curing for sample C3P1. This may be due to the different furnace in which the PCS was cured, where the weight gain after curing was 14.8% compared to 12.8% obtained in the preliminary work using smaller samples and furnace. The furnace used for pyrolysis was also different, being larger than that used in the preliminary work. The differences in the results showed the sensitivity of the PCS to the pyrolysis atmosphere. In the work of Hasegawa [3], the weight loss of oxidation-cured Mark I-type PCS, which appears to be similar to the present PCS, was followed by thermogravimetry in nitrogen. A pyrolysis yield of about 82 wt% was indicated at 1200 °C. Compared to this, the yields shown in Table VI seem very high even though the curing conditions used by Hasegawa were not reported. The replacement of network carbon such as Si-C-Si by oxygen during pyrolysis could produce a highly cross-linked structure with Si-O-Si bonds, leading to a high yield. Oxygen in the pyrolysis atmosphere is likely as leakage was possible in the furnace used.

TABLE VI The change in pyrolytic yield with pyrolysis temperature in argon

Sample	Pyrolysis Temperature (°C)	Pyrolysis yield (%)
C2P12	1200	98.0
C2P14	1400	96.4
C2P15	1500	95.0

Results of the elemental analysis and the calculated empirical formula of the pyrolytic residues are shown in Table VII. Two analyses were undertaken with sample C2P12 to obtain an indication of variation in the results. It can be seen that the carbon analyses were fairly consistent but there were variations of the order of 5% in the silicon and oxygen analyses.

Overall, the higher amount of oxygen in the residues was consistent with the higher amount of curing compared to the lower amount of curing received by the preliminary samples (Table V). A relative increase in the amount of carbon from sample C2P12 to C2P14 may be interpreted from these results, since the precipitation rate of free carbon from the silicon oxycarbide phase has been reported to be higher than the loss rate of carbon from the sample as gaseous CO below 1500 °C [12]. At 1500 °C, the loss rate of carbon was reported

TABLE VII Chemical composition (wt.%) and empirical formula of samples C2P12, C2P14 and C2P15

Sample	Si	C	O	Empirical formula
C2P12	50.5	27.1	22.4	$SiC_{1.25}O_{0.78}$
	50.8	24.7	24.5	$SiC_{1.14}O_{0.90}$
C2P14	51.0	23.7	26.4	$SiC_{1.16}O_{0.78}$
C2P15	52.6	24.9	22.5	$SiC_{1.11}O_{0.75}$

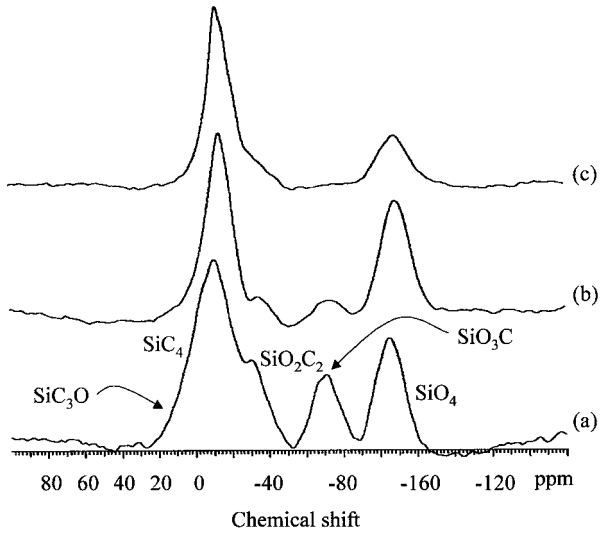

Figure 8 ^{29}Si DE/MAS NMR spectra of (a) C2P12; (b) C2P14; (c) C2P15.

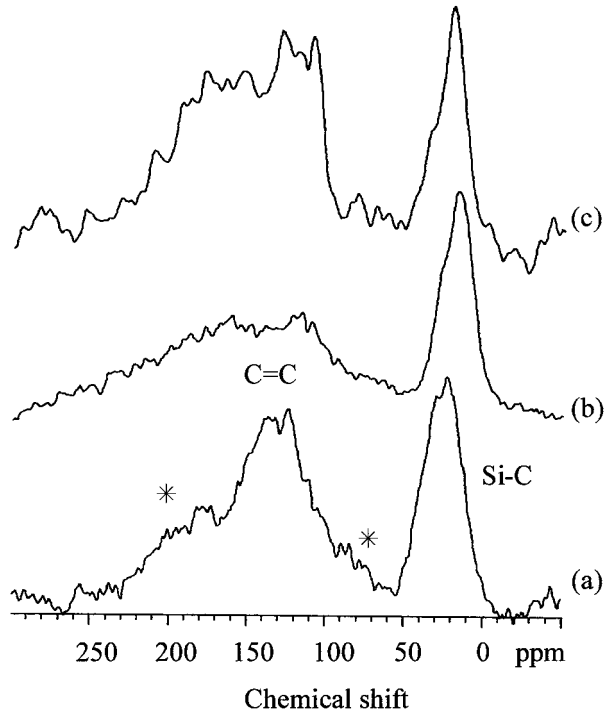

Figure 9 ^{13}C DE/MAS NMR spectra of (a) C2P12; (b) C2P14; (c) C2P15. * denotes a CSA spinning sideband.

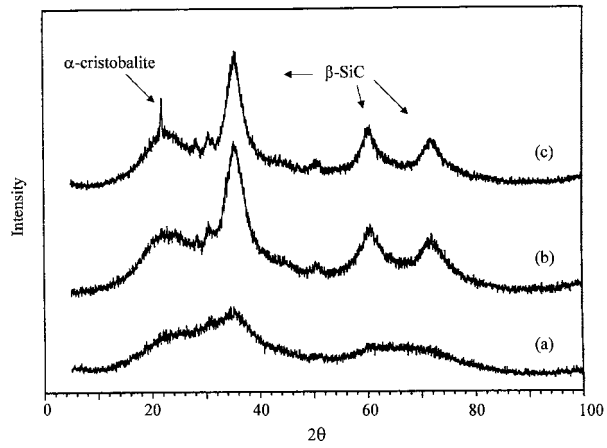

Figure 10 XRD patterns of (a) C2P12; (b) C2P14; (c) C2P15.

to be higher than the gain in carbon precipitation, hence the decreased amount of carbon found at 1500 °C in this study may be assumed to be true. No residual hydrogen was detected.

Fig. 8 shows are the ^{29}Si DE/MAS NMR spectra of the pyrolysis products C2P12 to C2P15. The main peak centered around −14 ppm was due to the resonance of β-SiC. It can be seen that the line width of this β-SiC peak became narrower with increasing pyrolysis temperature from sample C2P12 to C2P15, indicating an increase in the β-SiC crystallite size [6, 14]. A shift in the position of the β-SiC peak towards more negative values with increasing pyrolysis temperature was also observed, due to a more ordered state of the β-SiC. The presence of SiC_3O, SiC_2O_2, $SiCO_3$ and SiO_4 units gives rise to the signals at around +15, −30, −75 and −110 ppm, respectively. The signal due to SiC_3O units appears to have diminished with increasing pyrolysis temperature. This was, however, difficult to resolve as it may be obscured by the main SiC_4 peak. It can be seen, by comparing sample C2P12 (Fig. 8a) and C2P1 (Fig. 5b), that the relative proportions of SiO_4 and SiO_3 units are higher in sample C2P12 than in sample C2P1. Sample C2P12 had a high extent of curing and was pyrolyzed at a higher temperature than sample C2P1. This may suggest that the higher amount of oxygen or higher O/Si ratio introduced into sample C2P12 in the curing process could favour the oxygen-rich sites, where the silicon oxycarbide sites were consumed with formation of more SiO_4 sites as the temperature increased. With increasing pyrolysis temperature up to 1500 °C, the proportion of SiC_2O_2 and $SiCO_3$ structural units decreased. While the proportion of these oxycarbide units decreased, the proportion of the SiO_4 sites was found to have increased at 140 °C. At the same time, the proportion of the β-SiC phase increased. This seems to suggest that with increasing pyrolysis temperature above 1200 up to 1400 °C, the SiC_3O, SiC_2O_2 and $SiCO_3$ environments may redistribute as diffusion increases, favouring the separation of SiC (SiC_4) and SiO_2 (SiO_4) from these oxycarbide environments. This is consistent with the decomposition of the silicon oxycarbide phase producing β-SiC [11, 12]. By 1500 °C, the loss of some SiO_4 units was indicated by a reduction in the proportion of the peak at −110 ppm.

The ^{13}C DE/MAS NMR spectra of these residues are shown in Fig. 9. The interpretation of these spectra is similar to that of the spectra in Fig. 7 discussed above. The amount of free carbon may, however, be expected to increase with increasing temperature up to 1400 °C as free carbon precipitated from the silicon oxycarbide phase as discussed in the elemental analysis results. With increasing temperature above 1400 °C, the free carbon may be reduced as reaction with oxide phases can occur. This would be consistent with reduction in the carbon content in the elemental analysis.

The evolution in the XRD pattern with increasing pyrolysis temperature, i.e. from sample C2P12 to C2P15, is shown in Fig. 10. After pyrolyzing the cured PCS at 1200 °C (Fig. 10a), a broad diffraction pattern resembling that for β-SiC was seen, indicating a more

amorphous state of this sample. After pyrolysis at 1400 °C, the residue gave a more defined XRD pattern (Fig. 10b) showing major peaks at $2\theta = 36$, 60 and 72° corresponding to the (111), (220) and (311) diffraction lines of β-SiC. In addition, a broad peak appeared at $2\theta = 22°$ resembling the (101) line of α-cristobalite, showing the presence of micro-crystalline silica. This corresponded to the SiO_4 units already found in the ^{29}Si NMR results and the suggested phase separation of silica from the SiO_xC_y phase. After pyrolysis at 1200 °C (Fig. 10a) and at 1000°C (Fig. 7b), this silica peak was not apparent, although the presence of SiO_4 units was indicated in the ^{29}Si NMR results, hence the existence of amorphous silica in the 1000 and 1200 °C pyrolytic residues may be possible. In the present study, however, the SiO_4 units are assumed to be part of the SiO_xC_y phase below 1400 °C as found in more recent reports [27, 38, 48]. With increasing pyrolysis temperature at 1500 °C (Fig. 10c), the line width of the β-SiC peaks appeared similar to that found for the 1400 °C residue, but a sharper peak was observed co-existing with the broad peak at $2\theta = 22°$. This indicated the crystallization of α-cristobalite from the amorphous silica found in the 1400 °C residue.

Table III gives a summary of the products found in the present study from pyrolysis of cured PCS up to 1500 °C in argon compared to reported findings in literature where similar processing conditions have been used. The products found in the present study at 1200 °C were found to be similar to those reported in the literature [18, 50] at the same pyrolysis temperature. The products in the pyrolysis residues at 1400 and 1500 °C were not specified in the literature so no comparison was possible. The phase separation of β-SiC and SiO_2 from the SiO_xC_y phase with increasing temperature above ~1400 °C has been reported [16, 51, 52] however, but there is no mention of the evolution of the SiO_2 phase under the present pyrolysis conditions. The α-cristobalite found in the present study could have a negative effect on the high temperature strength of the ceramic if raised above 1400 °C, as cracking can occur on cooling due to large volume changes associated with the transition of the high to low form of cristobalite [53]. At 1500 °C, the decrease in the amounts of the SiO_xC_y phase, the SiO_2 phase and free carbon with a relative increase of the β-SiC phase is consistent with the general theory that the oxide species and carbon can react leading to the formation of silicon carbide. The silica phase may have been consumed by the reactions [54–56]:

$$SiO_2(s) + C(s) \rightarrow SiO(g) + CO(g)$$
$$SiO_2(s) + 3C(s) \rightarrow SiC(s) + 2CO(g)$$

3.1.4. Pyrolysis of cured PCS in vacuum

C2-cured PCS was pyrolyzed in vacuum to temperatures of 1000, 1200 and 1600 °C resulting in samples (VC2P10), (VC2P12) and (VC2P16), respectively. Table VIII lists the pyrolysis yields. At a similar pyrolysis temperature, the yield resulting from pyrolysis in vacuum was found to be lower than that pyrolyzed under argon flow. This should be attributed to the enhancement of the oxidation of free carbon, and of the forward decomposition reaction of the silicon oxycarbide phase [57] due to removal of the gaseous CO and SiO species from the vacuum furnace:

$$2SiC_xO_y\,(s) \rightarrow (1 + x - y)SiC\,(s) + (x + y - 1)CO\,(g) + (1 - x + y)SiO\,(g) \quad (1)$$

TABLE VIII The change in pyrolytic yield with pyrolysis temperature in vacuum

Sample	Pyrolysis Temperature (°C)	Pyrolysis yield (%)
VC2P10	1000	90.8
VC2P12	1200	76.3
VC2P16	1600	49.5

TABLE IX Chemical composition (wt.%) and empirical formula of cured samples pyrolyzed in vacuum

Sample	Si	C	H	O	Empirical formula
VC2P10	51.7	25.6	0.2	22.5	$SiC_{1.16}H_{0.11}O_{0.76}$
	50.9	25.5	0.1	23.5	$SiC_{1.17}H_{0.06}O_{0.81}$
VC2P12	55.4	27.2	0	17.4	$SiC_{1.15}H_{0.55}$
VC2P16	66.6	28.8	0	4.6	$SiC_{1.01}O_{0.12}$

Table IX shows the results of elemental analysis and the empirical formula of the vacuum pyrolyzed residues. Two analyses were undertaken with sample VC2P10 to give an indication of the variation in these results. Residual hydrogen was found in the product of pyrolysis at 1000 °C, indicating an incomplete conversion reaction where hydrogen was lost via condensation reactions between hydrocarbon groups such as CH_3 and CH_2 [50]. With increasing pyrolysis temperature, no residual hydrogen was detected and the excess carbon and oxygen are also reduced due to reactions between the excess carbon and SiO species. After pyrolysis at 1600 °C, the results indicated an almost stoichiometric SiC product. By comparing these results of pyrolysis in vacuum (Table IX) with those pyrolyzed in argon flow (Table VII), the loss of excess carbon and oxygen appears to be delayed in pyrolysis under argon compared to pyrolysis in vacuum. These results show that at a similar pyrolysis temperature, a more stoichiometric SiC product was obtained when pyrolyzed in vacuum than when pyrolyzed in argon flow. This is consistent with the removal of the gaseous SiO and CO species from the vacuum chamber, thus favouring the forward reaction in Equation 1, where the silicon oxycarbide phase is decomposed to give silicon carbide as the solid phase.

The ^{29}Si DE/MAS NMR spectra of the vacuum-pyrolyzed products are shown in Fig. 11. In the spectrum of the 1000 °C pyrolyzed residue (Fig. 11a) the main signal at −8 ppm was due to the presence of β-SiC. The signals centered around +15, −30 and −72 ppm were due to the silicon oxycarbide sites of SiC_3O, SiO_2C_2 and $SiCO_3$ respectively. SiO_4 units gave rise to the peak at −107 ppm. With increasing pyrolysis temperature, the β-SiC peak at −8 ppm in the 1000 °C spectra became narrower and moved to higher values of chemical shift at ca. −16 ppm in the spectrum of

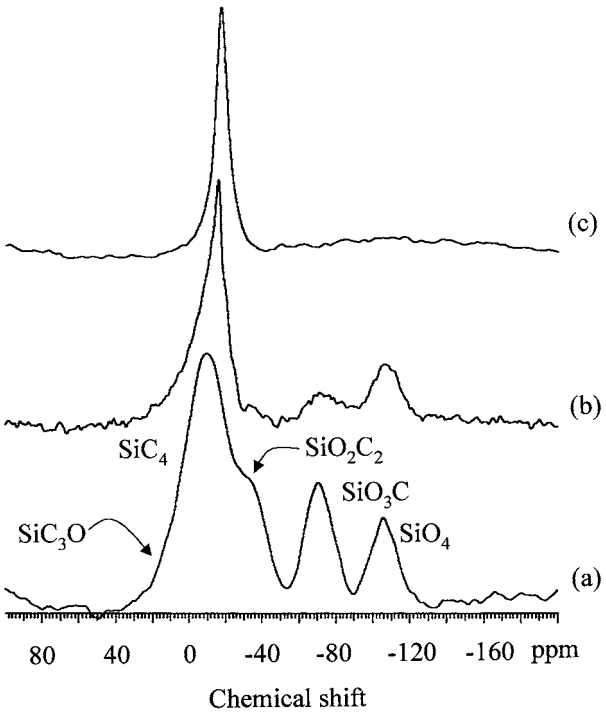

Figure 11 ^{29}Si DE/MAS NMR spectra of (a) VC2P10; (b) VC2P12; (c) VC2P16.

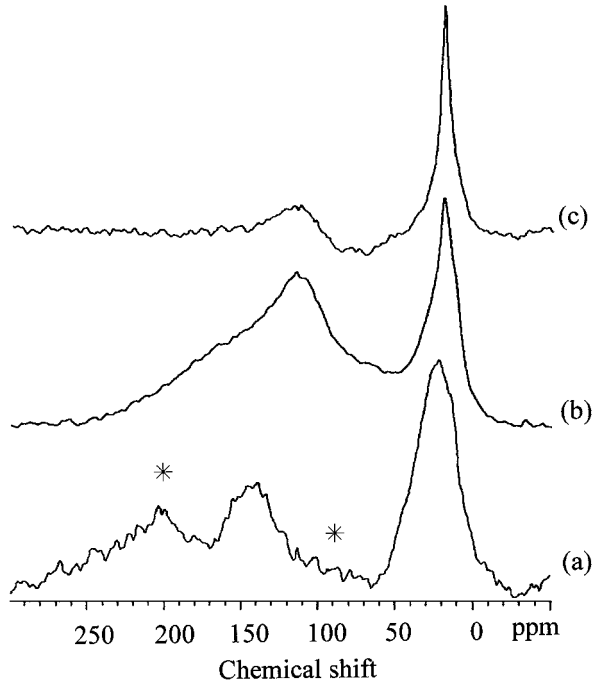

Figure 12 ^{13}C DS/MAS NMR spectra of (a) VC2P10; (b) VC2P12; (c) VC2P16. * denotes a CSA spinning sideband.

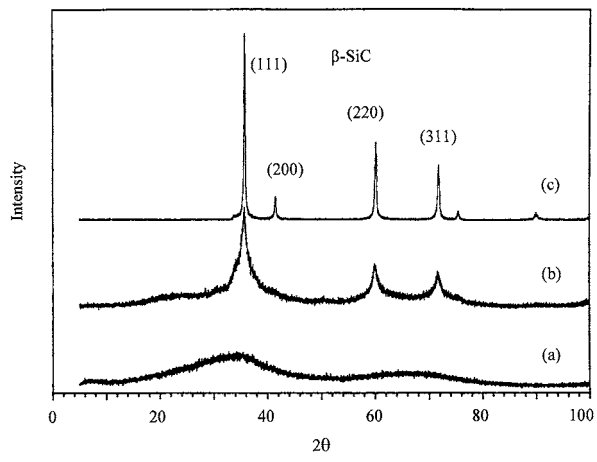

Figure 13 XRD pattern of (a) VC2P10; (b) VC2P12; (c) VC2P16.

the 1600 °C pyrolyzed residue (Fig. 11c). This was attributed to a more crystalline state of the β-SiC phase [6, 14]. It can also be seen that the proportion of the SiC_2O_2 and $SiCO_3$ peaks decreased with pyrolysis temperature while the proportion of the SiO_4 peak, i.e., the silica phase also decreased but to a lesser extent. After pyrolysis at 1600 °C, only the β-SiC peak at -16 ppm was apparent. Compared to a sample pyrolysed to a similar temperature of 1200 °C in argon (Fig. 8a), it can be seen that when the sample was heated in vacuum (Fig. 11b) the proportion of the oxide units was lower, while the proportion of β-SiC was higher. This was consistent with the reactions outlined above.

^{13}C DE/MAS NMR spectra of the vacuum-pyrolyzed products are shown in Fig. 12. The presence of unsaturated carbon nuclei in sample VC2P10 is shown by a CA spinning sideband at ca. 200 ppm, supporting the hydrogenated nature of the carbon as suggested in the elemental analysis result. The CSA spinning sidebands were not apparent in the samples VC2P12 or VC2P16, consistent with the near stoichiometric SiC composition suggested by the elemental analysis results. The β-SiC signal centered around +23 ppm narrowed with increasing crystallinity as the pyrolysis temperature increased.

The XRD patterns of the vacuum-pyrolyzed residues are shown in Fig. 13. The amorphous nature of the β-SiC phase in the 1000 °C−pyrolyzed residue was reflected by broad peaks (Fig. 13a). With increasing pyrolysis at 1200 °C, the peaks at $2\theta = 36$, 60 and 70° sharpened considerably due to crystallization of the β-SiC phase (Fig. 13b). A broad peak at $2\theta = 22°$ was due to amorphous silica. This amorphous silica peak resembling α-cristobalite was absent in the spectrum of the sample pyrolyzed at 1200 °C in argon (Fig. 10a). The β-SiC peaks in this vacuum-pyrolyzed sample were also sharper than in the argon-pyrolyzed sample. These findings were consistent with the enhancement of the microstructural evolution from the silicon oxycarbide species towards silicon carbide as discussed above. After pyrolysis at 1600 °C, the XRD pattern of the residue (Fig. 13c) appeared characteristic of the pattern for crystalline β-SiC. The peak at $2\theta = 22°$ was absent showing loss of the silica phase which agrees with the ^{29}Si NMR results.

Table III summarizes the products of pyrolysis of cured PCS in vacuum from the present study and those obtained by other authors where similar curing and pyrolysis conditions were used.

There appeared to be no further information in the literature on the products from pyrolysis in vacuum of cured PCS at temperatures used in this study. The PCS used in the work of Hasegawa [3] was reported to be the PC-470 type PCS pioneered by Yajima, hence is believed to be similar to the PCS used in the present study. The SiO_xC_y product was not mentioned by the author;

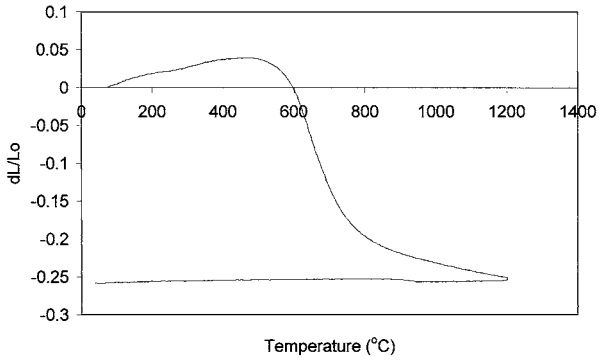

Figure 14 Thermal expansion of cured (C2) PCS pellet shown by the change in sample length with temperature at a heating/cooling rate of 100 °C (between room temperature and 1200 °C, held at 1200 °C for 1 h).

perhaps it was unidentifiable by the techniques used such as XRD as this product is amorphous. The quartz form of silica was found by Hasegawa [3] whereas α-cristobalite was identified in the present study. Again, differences in the precursor and thermal histories may explain the differences between the products found in the present study and those reported in the literature.

3.2. Thermal expansion

The thermal expansion of a pressed cured (C2) PCS powder, in the form of a disc, is shown in Fig. 14. The fractional change in length of the PCS disc with temperature is plotted on heating from room temperature to 1200 °C, where it was held for 1 h, and on cooling down to room temperature. As the temperature rose, the PCS polymer started to expand from about 75 °C and this expansion continued up to about 500 °C as the organic hydrocarbon groups decomposed. At about 500 °C, the sample began to contract, the rate of shrinkage becoming more rapid from 600 until about 800 °C. This temperature range during which the most rapid shrinkage occurs corresponded with the reported [2, 3] range during which the increase in density was most rapid, when the organic PCS transforms into a more inorganic state. By 800 °C, this organic to inorganic transition was almost complete, leading to an amorphous SiC-based product. This was reflected in the lower rate of shrinkage shown after 800 °C as the sample continued to sinter. During the one hour hold at 1200 °C, slow shrinkage continued and this irreversible shrinkage, due to formation of the ceramic state, was maintained on cooling down to room temperature. The overall reduction in the sample length was calculated to be 25.8%. From the dimensions of the sample before and after the dilatometry experiment, the volume of the sample was found to have decreased by about 56% after the dilatometry run.

4. Conclusions

Overall, the present study revealed the relationship between a series of processing conditions of the PCS and the pyrolysis product composition/structure. A number of these conditions have not been investigated in the literature. When processing conditions reported in the literature are believed to have been similar to that used in the present study, the products reported in the present study generally agreed with literature findings. Some of the products reported, however, were different to those found in the present study. Pyrolysis of uncured PCS at 1000 °C in the pyrolysis experiment produced silica as a minor product with no residual hydrogen whereas no silica but residual hydrogen was reported in the literature [6]. The amorphous silicon oxycarbide (SiO_xC_y) phase in the products of pyrolysis of cured PCS was not reported in the earlier literature. This may be due to its amorphous state leading to it not being observed by XRD used in their study and differences in the processing conditions or thermal histories.

Table III gives a summary of the solid products found in the present pyrolysis experiments and those reported in literature, where available.

Acknowledgements

H. Q. Ly acknowledges the support of EPSRC.

References

1. H. Q. LY, R. TAYLOR, R. J. DAY and F. HEATLEY, *J. Mater. Sci.* **36** (2001) 4037.
2. Y. HASEGAWA and K. OKAMURA, *J. Mater. Sci.* **18** (1983) 3633.
3. Y. HASEGAWA, *ibid.* **24** (1989) 1177.
4. M. TAKI, K. INUI, K. OKAMURA and M. SATO, *J. Mater. Sci. Lett.* **8** (1989) 918.
5. G. SORARU, F. BABONNEAU and J. D. MACKENZIE, *J. Non-Cryst. Solids* **106** (1988) 256.
6. *Idem.*, *J. Mater. Sci.* **25** (1990) 3886.
7. E. BOUILLON, F. LANGLAIS, R. PAILLER, R. NASLAIN, F. CRUEGE, P. V. HUONG, J. C. SARTHOU, A. DELPUECH, C. LAFFON, P. LAGARDE, M. MONTHIOUX and A. OBERLIN, *J. Mat. Sci.* **26** (1991) 1333.
8. S. J. TING, C. J. CHU and J. D. MACKENZIE, *J. Mater. Res.* **7** (1992) 164.
9. M. MONTHIOUX and O. DELVERDIER, *J. Eur. Ceram. Soc.* **16** (1996) 721.
10. K. OKAMURA, M. SATO, T. MATSUZAWA and Y. HASEGAWA, in "3rd Int. Conf. on Ultrastructure Processing of Ceramics, Glasses and Composites" (1987) pp. 501–518.
11. E. BOUILLON, D. MOCAER, J. F. VILLENEUVE, R. PAILLER, R. NASLAIN, M. MONTHIOUX, A. OBERLIN, C. GUIMON and G. PFISTER, *J. Mater. Sci.* **26** (1991) 1517.
12. Y. SASAKI, Y. NISHINA, M. SATO and K. OKAMURA, *J. Mater. Sci.* **22** (1987) 443.
13. J. LIPOWITZ and G. L. TURNER, *Abstracts of Papers of the American Chemical Society* **195** (1988) 74.
14. K. R. CARDUNER, G. R. HATFIELD, W. A. ELLINGSON and S. L. DIECKMAN, in "Handbook of Ceramics and Composites," Vol. 2, Mechanical Properties and Speciality Applications, edited by N. P. Cheremisinoff (Marcel Dekker, 1992) p. 465.
15. K. OKAMURA, M. SATO and Y. HASEGAWA, *J. Mater. Sci. Lett.* **2** (1983) 769.
16. B. A. BENDER, R. W. RICE and J. R. SPANN, *J. Amer. Ceram. Soc.* **70** (1987) C-58.
17. R. J. DAY, V. PIDDOCK, R. TAYLOR, R. J. YOUNG and M. ZAKIKHANI, *J. Mater. Sci.* **24** (1989) 2898.
18. G. R. HATFIELD and K. R. CARDUNER, *ibid.* **24** (1989) 4209.
19. T. ISHIKAWA, *Comp. Sci. Technol.* **51** (1994) 135.
20. Y. MANIETTE and A. OBERLIN, *J. Mater. Sci.* **24** (1989) 3361.
21. Y. XU, A. ZANGVIL, J. LIPOWITZ, J. A. RABE and G. A. ZANK, *J. Amer. Ceram. Soc.* **76** (1993) 3034.

22. L. C. SAWYER, M. JAMIESON, D. BRIKOWSKI, M. ISHAQ HAIDER and R. T. CHEN, *J. Amer. Ceram. Soc.* **70** (1987) 798.
23. L. C. SAWYER, R. ARONS, F. HAIMBACH, M. JAFFE and K. D. RAPPAPORT, *Ceram. Eng. Sci. Proc.* **6** (1985) 567.
24. S. YAJIMA, K. OKAMURA, T. MATSUZAWA, Y. HASEGAWA and T. SHISHIDO, *Nature* **279** (1979) 706.
25. A. R. BUNSELL and M. H. BERGER, *Comp. Sci. Technol.* **51** (1994) 127.
26. L. PORTE and A. SARTRE, *J. Mater. Sci.* **24** (1989) 271.
27. C. LAFFON, A. M. FLANK, P. LAGARDE, M. LARIDJANI, R. HAGEGE, P. OLRY, J. COTTERET, J. DIXMIER, J. L. MIQUEL, H. HOMMEL and A. P. LEGRAND, *ibid.* **24** (1989) 1503.
28. P. SCHRECK, C. VIX-GUTERL, P. EHRBURGER and J. LAHAYE, *ibid.* **27** (1992) 4243.
29. S. M. BLEAY, A. R. CHAPMAN, G. LOVE and V. D. SCOTT, *ibid.* **27** (1992) 5389.
30. P. LE COUSTUMER, M. MONTHIOUX and A. OBERLIN, *J. Eur. Ceram. Soc.* **11** (1993) 95.
31. B. HAHN, R. WEISSMANN and P. GREIL, *J. Mater. Sci. Lett.* **15** (1996) 1243.
32. J. LIPOWITZ, H. A. FREEMAN, R. T. CHEN and E. R. PRACK, *Adv. Ceram. Mater.* **2** (1987) 121.
33. H. ZHANG and C. G. PANTANO, *J. Amer. Ceram. Soc.* **73** (1990) 958.
34. R. PAMPUCH, W. PTAK, S. JONAS and J. STOCH, *Mater. Sci. Monographs* **6** (1980) 435.
35. G. M. RENLUND, S. PROCHAZKA and R. H. DOREMUS, *J. Mater. Res.* **6** (1991) 2716.
36. F. BABONNEAU, G. D. SORARU, G. D'ANDREA, S. DIRE and L. BOIS, *Mater. Res. Soc. Symp. Proc.* **271** (1992) 789.
37. G. M. RENLUND, S. PROCHAZKA and R. H. DOREMUS, *J. Mater. Res.* **6** (1991) 2723.
38. R. J. P. CORRIU, D. LECLERCQ, P. H. MUTIN and A. VIOUX, *J. Mater. Sci.* **30** (1995) 2313.
39. O. DELVERDIER, M. MONTHIOUX, D. MOCAER and R. PAILLER, *J. Eur. Ceram. Soc.* **12** (1993) 27.
40. H. YAO, S. KOVENKLIOGLU and D. M. KALYON, *Chem. Eng. Comm.* **96** (1990) 155.
41. M. NARISAWA, S. ODA, S. KITANO and K. OKAMURA, *J. Appl. Polym. Sci.* **65** (1997) 261.
42. R. M. SILVERSTEIN, G. CLAYTON BASSLER and T. C. MORRILL, "Spectrometric Identification of Organic Compounds," 5th edn. (Wiley, New York, 1991).
43. N. HOCHET, M. H. BERGER and A. R. BUNSELL, *J. Microsc. Oxford* **185** (1997) 243.
44. H. P. MARTIN, G. IRMER, G. SCHUSTER and E. MULLER, *Fresenius J. Anal. Chem.* **349** (1994) 160.
45. Z. F. ZHANG, F. BABONNEAU, R. M. LAINE, Y. MU, J. F. HARROD and J. A. RAHN, *J. Amer. Ceram. Soc.* **74** (1991) 670.
46. E. LIPPMAA, M. MAGI, A. SAMOSON, G. ENGELHARDT and A. R. GRIMMER, *J. Amer. Chem. Soc.* **102** (1980) 4889.
47. G. D. SORARU, G. D'ANDREA, R. CAMPOSTRINI, F. BABONNEAU and G. MARIOTTO, *J. Amer. Ceram. Soc.* **78** (1995) 379.
48. A. T. HEMIDA, R. PAILLER and R. NASLAIN, *J. Mater. Sci.* **32** (1997) 2359.
49. S. YAJIMA, *Ceram. Bull.* **62** (1983) 893.
50. R. BODET, N. JIA and R. E. TRESSLER, *J. Eur. Ceram. Soc.* **16** (1996) 653.
51. T. F. COOKE, *J. Amer. Ceram. Soc.* **74** (1991) 2959.
52. M. MONTHIOUX, D. COJEAN, O. DELVERDIER, P. LECOUSTUMER and V. MADIGOU, *Microsc. Microanal. Microstruct.* **2** (1991) 47.
53. W. D. KINGERY, "Introduction to Ceramics," 2nd edn. (Wiley-Interscience, 1976), p. 87.
54. V. G. GERLIVANOV, R. A. RABINOVITCH, N. M. BALAGUROVA and N. N. KORNEEV, "Residual Stresses, II: Science and Technology," Vol. 1 (Elsevier Science, UK, 1992), p. 567.
55. C. H. ANDERSSON and R. WARREN, *Composites* **15** (1984) 16.
56. V. D. KRSTIC, *J. Amer. Ceram. Soc.* **75** (1992) 170.
57. R. BODET, N. JIA and R. E. TRESSLER, *J. Eur. Ceram. Soc.* **15** (1995) 997.

Received 14 April 1999
and accepted 24 October 2000